LA-UR-15-26879
Approved for public release; distribution is unlimited.

Title: A High-Order Central ENO Method for ALE Simulation of Three-Dimensional Compressible Flows

Author(s): Charest, Marc Robert Joseph
Canfield, Thomas R.
Morgan, Nathaniel Ray
Waltz, Jacob I.
Wohlbier, John Greaton

Intended for: MultiMat 2015, 2015-09-07 (Wurzburg, Germany)

Issued: 2015-09-01

A High-Order Central ENO Method for ALE Simulation of Three-Dimensional Compressible Flows

Marc R.J. Charest
Thomas R. Canfield
Nathaniel R. Morgan
Jacob Waltz
John G. Wohlbier

MultiMat 2015
Würzburg, Germany
Sept 7–11, 2015

Target Applications

Multi-Material Shock Physics (ALE)

- Inertial confinement fusion (ICF)
- Materials science experiments
- Armor/target penetration
- Rayleigh-Taylor instabilities

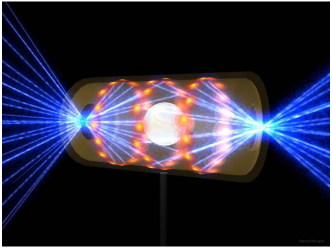

Fluid Dynamics with Moving Interfaces/Domains

- Shuttle launch/re-entry dynamics
- Store separation
- Rotating propellers

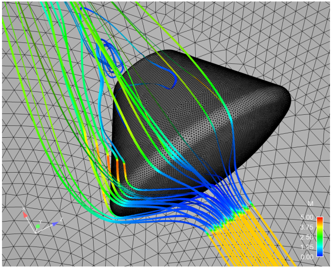

What are high-order methods?

- Used to improve the spatial/temporal representation of numerical solutions
- Advanced interpolants (usually polynomials) of accuracy higher than second-order

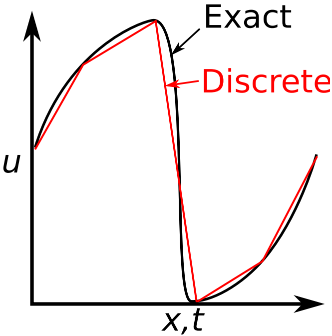

What are high-order methods?

- Used to improve the spatial/temporal representation of numerical solutions
- Advanced interpolants (usually polynomials) of accuracy higher than second-order

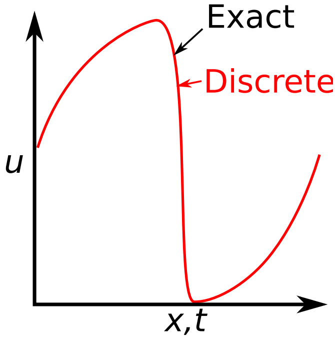

What are high-order methods?

- Used to improve the spatial/temporal representation of numerical solutions
- Advanced interpolants (usually polynomials) of accuracy higher than second-order
- Can be unstable/oscillatory → produces unphysical solutions

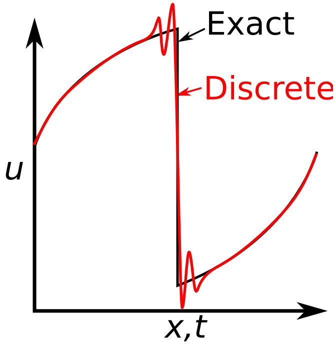

High-Order Accurate Discretization Methods

Higher accuracy for the same mesh size

- Capture wave-propagation phenomena (shocks & rarefaction waves, contact surfaces)
- Capture varying scales
- Model complex geometries (irregular & curved boundaries)

Computational savings for the same accuracy requirements

- Unsteady flows
- Large numbers of solution variables (complex chemistry, radiation)

More work per cell/node

- Well-suited for advanced architectures?

Arbitrary Lagrangian-Eulerian (ALE) Methods

ALE methods for hydrodynamics solve the hyperbolic time-dependent PDEs of the form:

$$\frac{\partial \mathbf{U}}{\partial t} + \vec{\nabla} \cdot \vec{\mathbf{F}}\left(\mathbf{U}\right) = \mathbf{S} \qquad \vec{x} \in \Omega(t) \subset \mathbb{R}^3$$

where the domain $\Omega(t)$ moves *arbitrarily*. There are two distinct limits:

- The mesh is stationary $\rightarrow$ Eulerian limit.
- The mesh moves with fluid $\rightarrow$ Lagrangian limit.

How do we combine with high-order methods. Challenges include:

- Preserving geometric conservation laws.
- Avoiding splitting errors.
- Maintaining stability, i.e., robust/monotone solutions.
- Achieving formal temporal/spatial accuracy.

Finite-Volume Formulation

General system of conservation laws for a time-dependent computational domain $\Omega(t)$

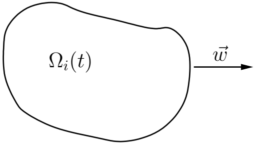

$$\frac{\partial \mathbf{U}}{\partial t} + \frac{\partial \mathbf{E}}{\partial x} + \frac{\partial \mathbf{F}}{\partial y} + \frac{\partial \mathbf{G}}{\partial z} = \mathbf{S}$$

Computational domain $\Omega(t)$ was sub-divided into smaller finite-sized control volumes, $\Omega_i(t)$

$$\Omega(t) = \bigcup \Omega_i(t)$$

Semi-discrete integral form for a **moving** control volume $\Omega_i(t)$

$$\frac{\mathrm{d}}{\mathrm{d}t}\left(|\Omega_i|\bar{\mathbf{U}}_i\right) = -\oint_{\partial\Omega_i(t)} \left(\vec{\mathbf{F}} - \mathbf{U} \otimes \vec{w}\right) \cdot \hat{n}\, \mathrm{d}\Gamma + \int_{\Omega_i(t)} \mathbf{S}\, \mathrm{d}\Omega$$

Tetrahedral mesh

- Easier to mesh complex domains

Unknowns associated with vertices

- Avoids stiffness-related issues encountered by cell-based ALE formulations
- Approximately six times fewer vertices than elements
- More nearest neighbors, i.e. larger compact supporting stencils

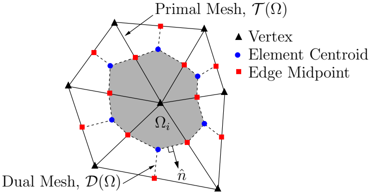

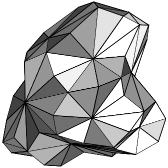

Sample dual volume

Tetrahedral mesh

- Easier to mesh complex domains

Unknowns associated with vertices

- Avoids stiffness-related issues encountered by cell-based ALE formulations
- Approximately six times fewer vertices than elements
- More nearest neighbors, i.e. larger compact supporting stencils

Other unstructured high-order 3D ALE schemes for hydrodynamics are cell-based

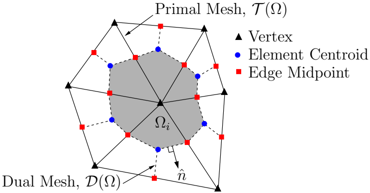

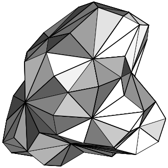

Sample dual volume

High-Order Spatial Discretization Procedure

Control volumes, Ω_i, and their surfaces, $\partial\Omega_i$, were sub-divided into tetrahedral and triangular segments

$$\Omega_i = \bigcup \mathrm{T}_t \qquad\qquad \partial\Omega_i = \bigcup \Gamma_s$$

Integrals discretized using standard Gaussian quadrature rules

$$\int_{\Omega_i} \mathbf{S}\, \mathsf{d}\Omega = \sum_t |\mathrm{T}_t| \sum_{q=1}^{N} \omega_q \mathbf{S}_q + \mathcal{O}\left(h^{r+1}\right)$$

$$\oint_{\partial\Omega_i} \vec{\mathbf{F}} \cdot \hat{n}\, \mathsf{d}\Gamma = \sum_s |\Gamma_s| \sum_{q=1}^{M} \left[\omega_q \vec{\mathbf{F}}_q \cdot \hat{n}_s\right] + \mathcal{O}\left(h^{r+1}\right)$$

N and $M > 1$ for $r > 1$

High-Order Piecewise Polynomial Interpolation

Based on k-exact reconstruction procedure of Barth (1993)

$$u(x,y,z) - P_i^k(x,y,z) = \mathcal{O}\left(h^{k+1}\right)$$

Reconstruct a piecewise polynomial approximation for the solution in each control volume Ω_i

$$P_i^k(x,y,z) = \sum_{p_1=0}^{p1+p2+p3\leq k}\sum_{p_2=0}\sum_{p_3=0}(x-x_i)^{p_1}(y-y_i)^{p_2}(z-z_i)^{p_3}D_{p_1p_2p_3}$$

Solve a least-squares problem for the polynomial coefficients $\mathbf{D} = \{D_{p_1p_2p_3}\}$, i.e., find $\mathbf{D}$ that minimizes

$$||\mathbf{AD} - \bar{\mathbf{U}}||_2$$

$\mathcal{N}_D = \frac{1}{6}(k+1)(k+2)(k+3)$ unknown coefficients

Hybrid Central ENO (CENO) Reconstruction

Problem:

- Polynomial interpolation can generate spurious oscillations.

Hybrid Central ENO (CENO) Reconstruction

Problem:

- Polynomial interpolation can generate spurious oscillations.

Solution: CENO Reconstruction

- Piecewise polynomial approximation in smooth regions:

$$P_i^k(x,y,z) = \sum_{p_1=0}^{p1+p2+p3\leq k}\sum_{p_2=0}\sum_{p_3=0}(x-x_i)^{p_1}(y-y_i)^{p_2}(z-z_i)^{p_3}D_{p_1p_2p_3}$$

- Limited piecewise linear approximation near discontinuities:

$$P_i^{k=1}(x,y,z) = \bar{u}_i + \phi_i\vec{\nabla}u\cdot(\vec{x}-\vec{x}_i)$$

- Use a smoothness indicator to switch between reconstruction procedures.

ALE Mesh Velocity

$$\frac{\mathsf{d}}{\mathsf{d}t}\left(|\Omega_i|\bar{\mathbf{U}}_i\right) = -\oint_{\partial\Omega_i(t)}\left(\vec{\mathbf{F}} - \mathbf{U}\otimes\vec{w}\right)\cdot\hat{n}\,\mathsf{d}\Gamma + \int_{\Omega_i(t)}\mathbf{S}\,\mathsf{d}\Omega$$

Arbitrary Lagrangian-Eulerian (ALE)

- $\vec{w} \neq \vec{0} \neq \vec{v}$
- Combine the advantages of both limits
- Use a Lagrangian reference as much as possible
- Revert towards an Eulerian reference to avoid mesh tangling
- Use *velocity-based* mesh smoothing

Velocity-Based Mesh Smoother

$$\frac{\mathsf{d}}{\mathsf{d}t}\left(|\Omega_i|\bar{\mathbf{U}}_i\right) = -\oint_{\partial\Omega_i(t)}\left(\vec{\mathbf{F}} - \mathbf{U}\otimes\vec{w}\right)\cdot\hat{n}\,\mathsf{d}\Gamma + \int_{\Omega_i(t)}\mathbf{S}\,\mathsf{d}\Omega$$

Procedure:

1. Discretize the mesh velocity field using *linear finite elements*
2. Use fluid velocity as initial guess for mesh velocity ($\vec{w}_0 = \vec{v}$)
3. Solve a Laplacian for a new smoothed velocity field

   $$\vec{\nabla}\cdot\left[\mu\vec{\nabla}\vec{w}(\vec{x},t)\right] = \vec{0}$$

   to a set *relative* tolerance ε.
4. Move vertices at new, smoothed velocity $\vec{w}$

Overall Solution Algorithm

Temporal evolution using high-order explicit RK:

Compute Δt^n and $\mathbf{Q}_i^n = |\Omega_i^n| \bar{\mathbf{U}}_i^n$.
foreach intermediate stage s **do**
    Reconstruct $\mathbf{U}\left(\vec{x},\, t^s\right)$.
    Compute $\left\{\vec{w}_j\left(t^s\right)\right\}$ analytically or using Laplacian-based smoother.
    Compute $\mathbf{R}_i^s = \mathrm{d}\mathbf{Q}_i^s / \mathrm{d}\, t$.
    Advance $\mathbf{Q}_i^s$ to $\mathbf{Q}_i^{s+1}$ using explicit RK time-marching.
    Recompute the geometric parameters of the new mesh, i.e., $|\Omega_i^{s+1}|$, based on new coordinates $\vec{x}_j^{s+1}$.
    Update solution, $\bar{\mathbf{U}}_i^{s+1} \leftarrow \mathbf{Q}_i^{s+1} \;/\; |\Omega_i^{s+1}|$.

Overall Solution Algorithm

Temporal evolution using high-order explicit RK:

Compute Δt^n and $\mathbf{Q}_i^n = |\Omega_i^n| \bar{\mathbf{U}}_i^n$.
foreach intermediate stage s **do**
    Reconstruct $\mathbf{U}\left(\vec{x},\, t^s\right)$.
    Compute $\{\vec{w}_j\left(t^s\right)\}$ analytically or using Laplacian-based smoother.
    Compute $\mathbf{R}_i^s = \mathrm{d}\mathbf{Q}_i^s / \mathrm{d}\, t$.
    Advance $\mathbf{Q}_i^s$ to $\mathbf{Q}_i^{s+1}$ using explicit RK time-marching.
    Recompute the geometric parameters of the new mesh, i.e., $|\Omega_i^{s+1}|$, based on new coordinates $\vec{x}_j^{s+1}$.
    Update solution, $\bar{\mathbf{U}}_i^{s+1} \leftarrow \mathbf{Q}_i^{s+1} \; / \; |\Omega_i^{s+1}|$.

This procedure guarantees geometric conservation

Governing Equations

Euler equations for compressible flows:

$$\frac{\partial \rho}{\partial t} + \vec{\nabla} \cdot (\rho \vec{v}) = S_\rho$$

$$\frac{\partial}{\partial t}(\rho \vec{v}) + \vec{\nabla} \cdot (\rho \vec{v}\vec{v} + p\vec{\mathbf{I}}) = \vec{S_v}$$

$$\frac{\partial}{\partial t}(\rho e_{\mathsf{t}}) + \vec{\nabla} \cdot (\rho \vec{v} e_{\mathsf{t}} + \vec{v} p) = S_e$$

$$e_{\mathsf{t}} = e + \frac{1}{2}\vec{v} \cdot \vec{v}$$

For an ideal gas, $p = (\gamma - 1)\rho e$.

Convection of an Isentropic Vortex

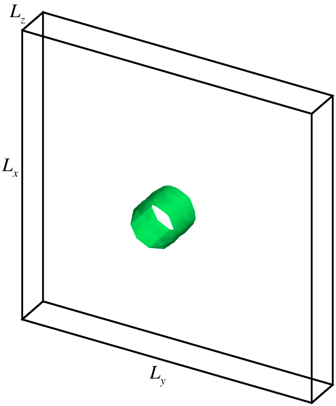

An initially uniform field is perturbed at time $t = 0\,\mathrm{s}$ by a cylindrical vortex

$$\delta T = \frac{(\gamma - 1)\beta^2}{8\gamma\pi^2} \exp\left(1 - r^2\right)$$

$$\delta u = -\frac{\beta}{2\pi}\overline{y} \exp\left(\frac{1 - r^2}{2}\right)$$

$$\delta v = \frac{\beta}{2\pi}\overline{x} \exp\left(\frac{1 - r^2}{2}\right)$$

$$\delta w = 0$$

Isentropic Vortex - Mesh Motion

Similar sinusoidal mesh motion

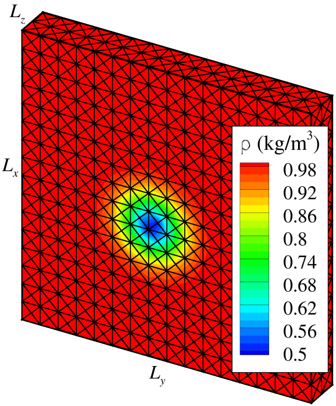

$t = 0\,\mathrm{s}$

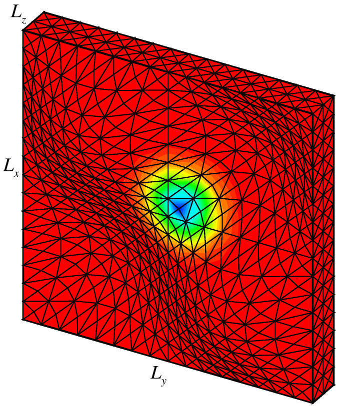

$t = t_{\max} = 0.1\,\mathrm{s}$

Isentropic Vortex - Temporal Error

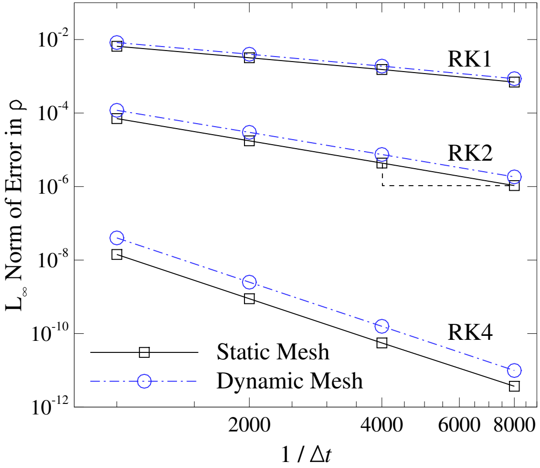

Isentropic Vortex - Spatial Error

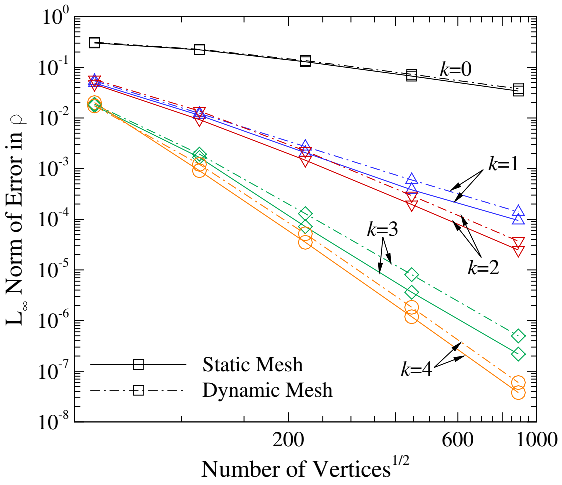

Isentropic Vortex - Computational Efficiency

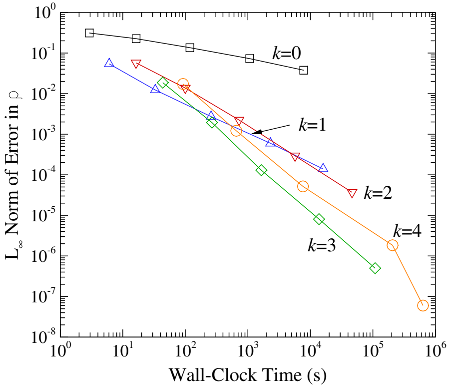

Moving Mesh

Smooth, adiabatic compression ($t < 0$) followed by expansion ($t > 0$) of an inviscid, polytropic ball of gas (Kidder, 1974).

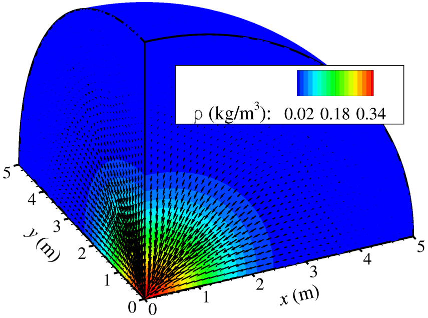

$$\rho(\vec{r},t) = \frac{\rho_0 R_0^3}{R^3(t)} \exp\left[-\frac{r^2}{R^2(t)}\right]$$

$$p(\vec{r},t) = \frac{\rho_0 R_0^3 \ddot{R}(t)}{2R^2(t)} \exp\left[-\frac{r^2}{R^2(t)}\right]$$

$$\vec{v}(\vec{r},t) = \frac{\dot{R}(t)}{R(t)}\vec{r}$$

where $\vec{r}$ is the radial position vector and $R(t)$ is the scale radius.

The Kidder Problem - Mesh Motion

Pressure contours, 145k Tetrahedra

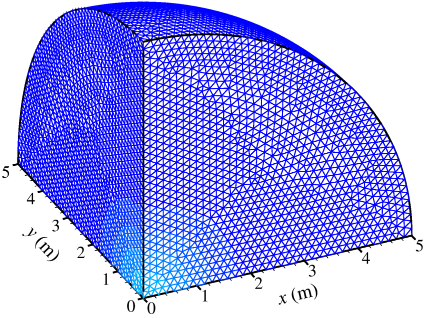

$t = \pm 1$ s

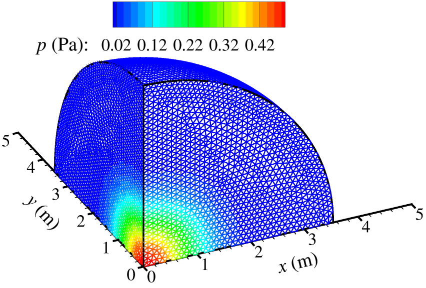

$t = 0$ s

The Kidder Problem - Reconstruction

Reconstructed density at each point

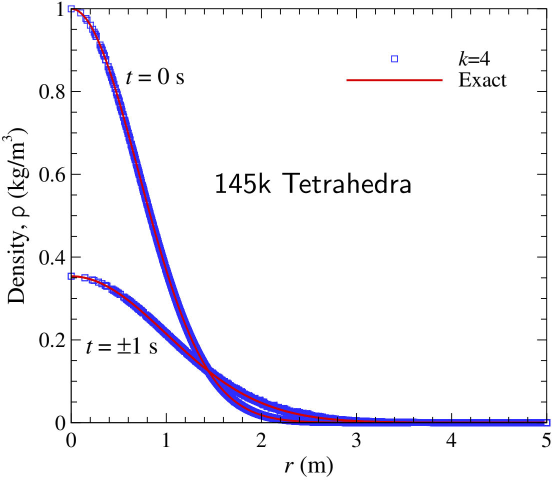

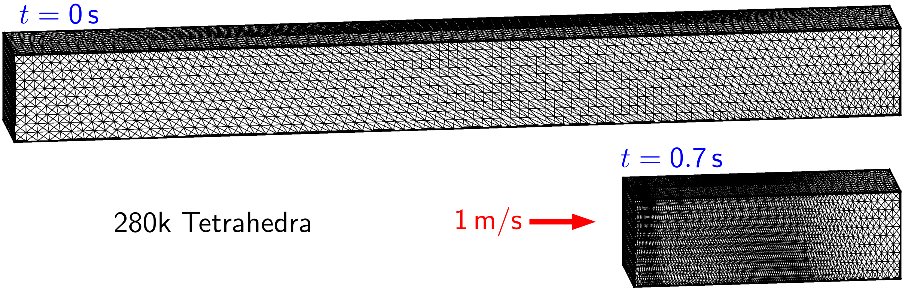

The channel initially contains a stationary fluid with $\gamma = 5/3$ and

$$\mathbf{W}(\vec{x},0) = \left[1\,\mathrm{kg/m^3},\ \vec{0}\,\mathrm{m/s},\ 10^{-6}\,\mathrm{Pa}\right]$$

Moving Piston - Density Contours

Final density contours at $t = 0.7\,\mathrm{s}$

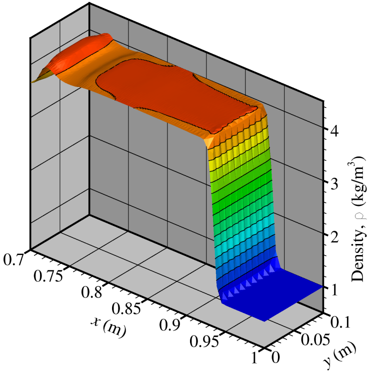

Uniform Mesh

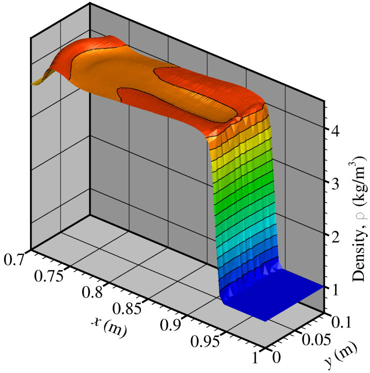

Skewed Mesh

An initial point source at the origin drives an outwardly propagating shock wave.

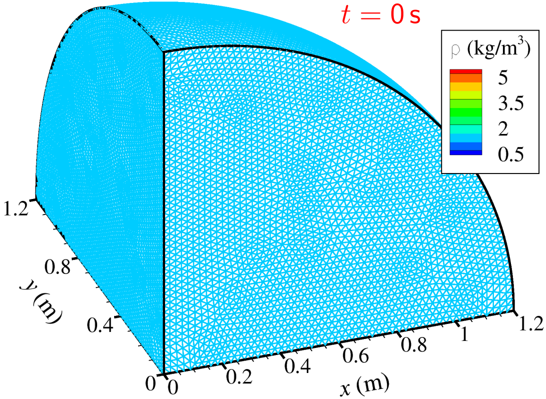

$$\rho(r,\,0) = 1\,\mathsf{kg/m^3}$$

$$\vec{v}(r,\,0) = \vec{0}\,\mathsf{m/s}$$

$$e(r,\,0) = \begin{cases} \dfrac{3\,e_{\mathsf{blast}}}{4\pi r_0^3}, & r \le r_0 \\ 0, & r > r_0 \end{cases}$$

where $r = \sqrt{x^2 + y^2 + z^2}$.

Sedov Blast Wave

An initial point source at the origin drives an outwardly propagating shock wave.

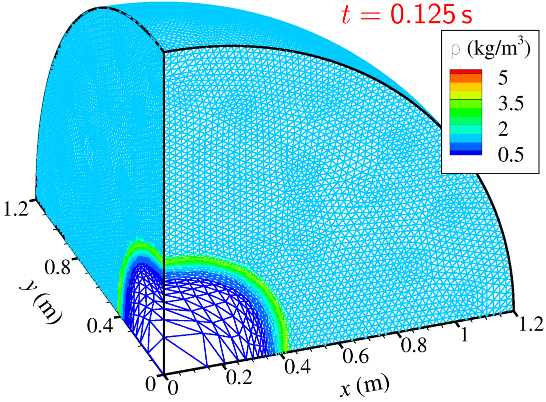

$$\rho(r,\,0) = 1\,\mathsf{kg/m}^3$$

$$\vec{v}(r,\,0) = \vec{0}\ \mathsf{m/s}$$

$$e(r,\,0) = \begin{cases} \dfrac{3\,e_{\mathsf{blast}}}{4\pi r_0^3}, & r \le r_0 \\ 0, & r > r_0 \end{cases}$$

where $r = \sqrt{x^2 + y^2 + z^2}$.

An initial point source at the origin drives an outwardly propagating shock wave.

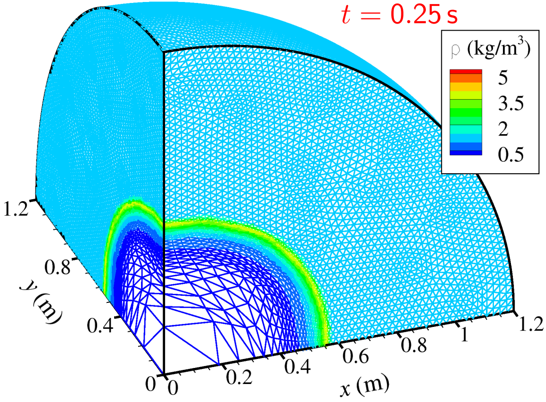

$$\rho(r,\,0) = 1\,\mathrm{kg/m^3}$$

$$\vec{v}(r,\,0) = \vec{0}\ \mathrm{m/s}$$

$$e(r,\,0) = \begin{cases} \dfrac{3\,e_{\mathrm{blast}}}{4\pi r_0^3}, & r \le r_0 \\ 0, & r > r_0 \end{cases}$$

where $r = \sqrt{x^2 + y^2 + z^2}$.

Sedov Blast Wave

An initial point source at the origin drives an outwardly propagating shock wave.

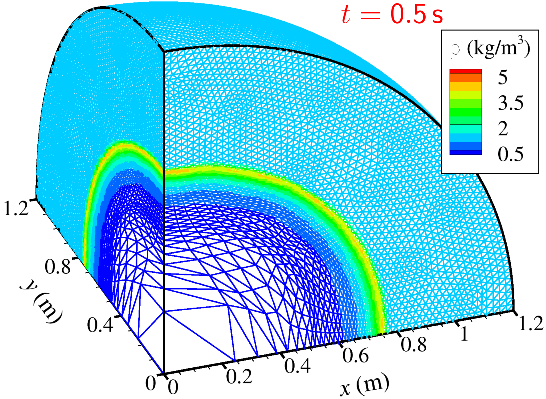

$$\rho(r,\,0) = 1\,\mathsf{kg/m^3}$$

$$\vec{v}(r,\,0) = \vec{0}\ \mathsf{m/s}$$

$$e(r,\,0) = \begin{cases} \dfrac{3\,e_{\mathsf{blast}}}{4\pi r_0^3}, & r \le r_0 \\ 0, & r > r_0 \end{cases}$$

where $r = \sqrt{x^2 + y^2 + z^2}$.

Sedov Blast Wave

An initial point source at the origin drives an outwardly propagating shock wave.

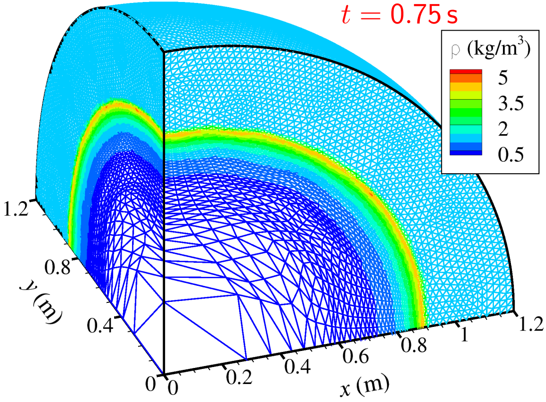

$$\rho(r,\,0) = 1\,\mathsf{kg/m}^3$$

$$\vec{v}(r,\,0) = \vec{0}\ \mathsf{m/s}$$

$$e(r,\,0) = \begin{cases} \dfrac{3\,e_{\mathsf{blast}}}{4\pi r_0^3}, & r \le r_0 \\ 0, & r > r_0 \end{cases}$$

where $r = \sqrt{x^2 + y^2 + z^2}$.

An initial point source at the origin drives an outwardly propagating shock wave.

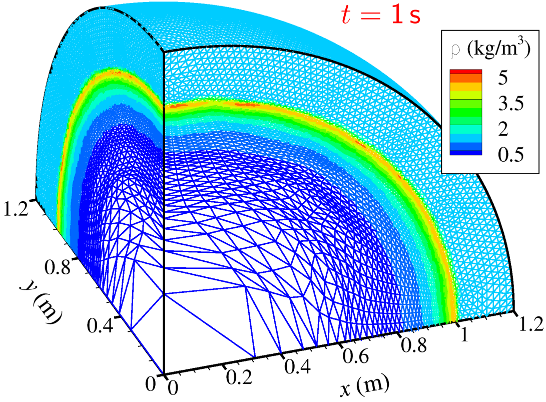

$$\rho(r,\,0) = 1\,\mathsf{kg/m^3}$$

$$\vec{v}(r,\,0) = \vec{0}\ \mathsf{m/s}$$

$$e(r,\,0) = \begin{cases} \dfrac{3\,e_{\mathsf{blast}}}{4\pi r_0^3}, & r \le r_0 \\ 0, & r > r_0 \end{cases}$$

where $r = \sqrt{x^2 + y^2 + z^2}$.

Sedov Blast Wave - Reconstruction

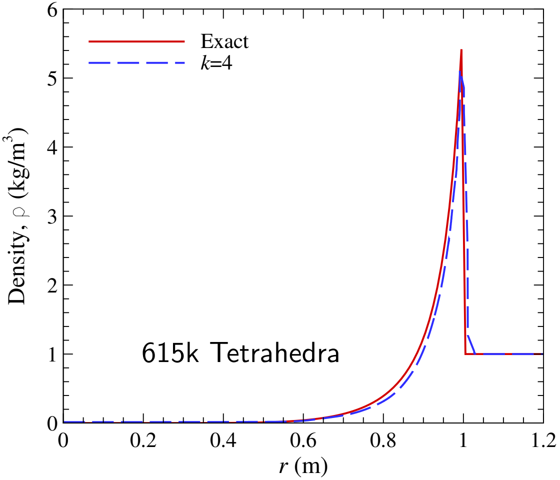

Sedov Blast Wave - Spherical Symmetry

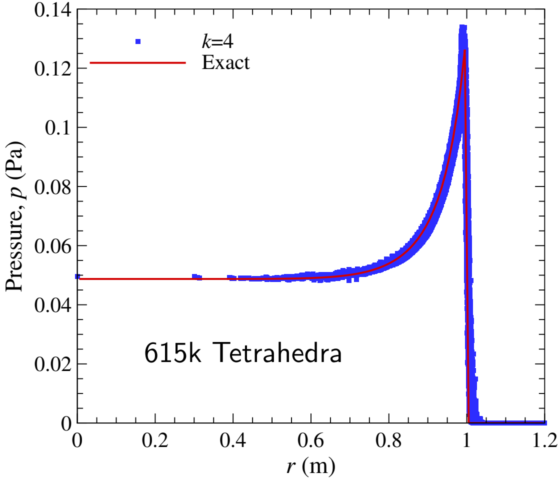

AMR Under Development

Sedov Blast Wave:

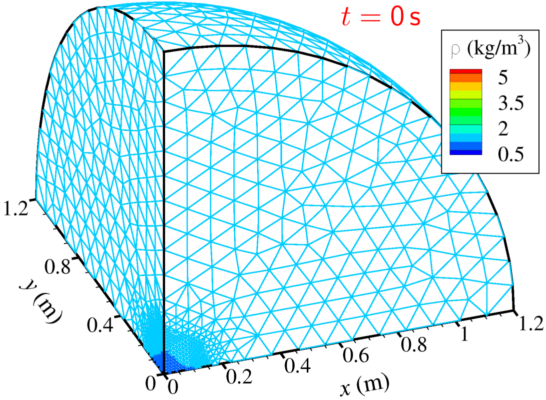

22655 Elements

Challenges:

- Maintain conservation *and* accuracy through prolongation/restriction

AMR Under Development

Sedov Blast Wave:

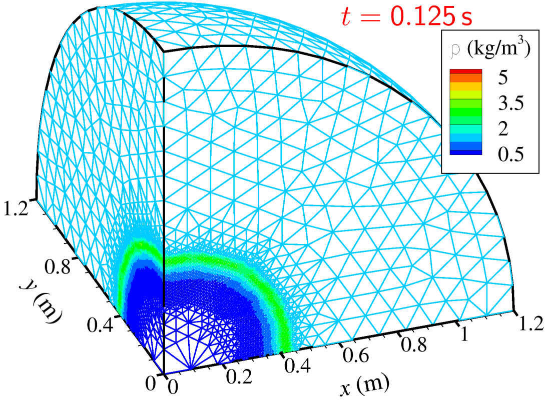

276671 Elements

Challenges:

- Maintain conservation *and* accuracy through prolongation/restriction

Sedov Blast Wave:

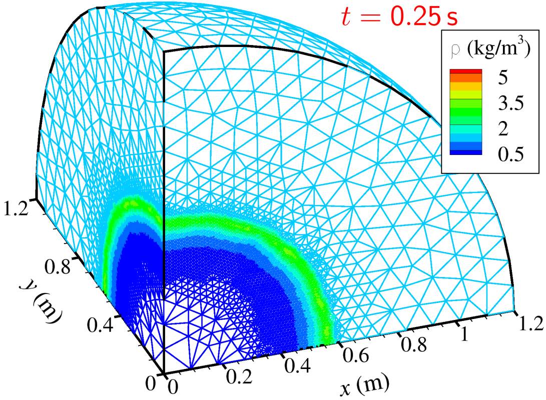

561580 Elements

Challenges:

- Maintain conservation *and* accuracy through prolongation/restriction

AMR Under Development

Sedov Blast Wave:

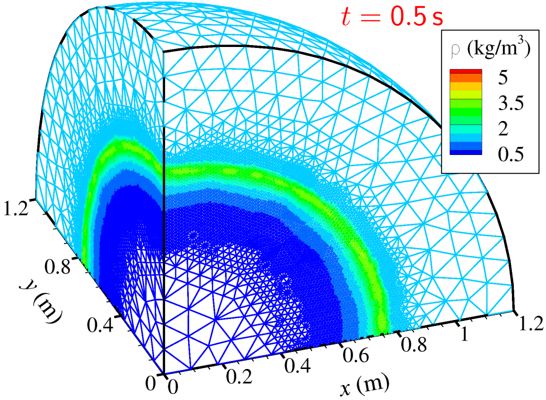

1307080 Elements

Challenges:

- Maintain conservation *and* accuracy through prolongation/restriction

AMR Under Development

Sedov Blast Wave:

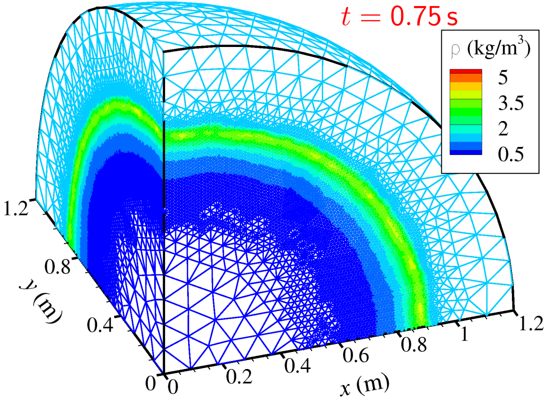

1779791 Elements

Challenges:

- Maintain conservation *and* accuracy through prolongation/restriction

Sedov Blast Wave:

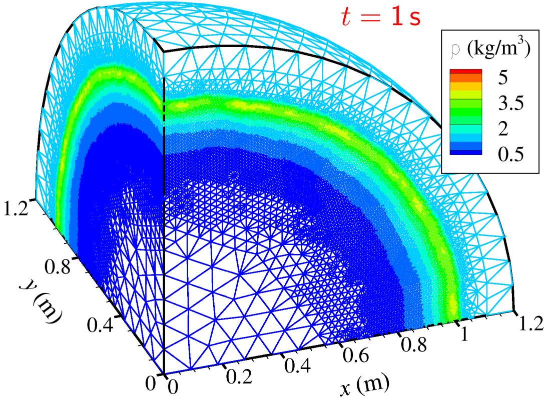

2273670 Elements

Challenges:

- Maintain conservation *and* accuracy through prolongation/restriction

Concluding Remarks & Future Research

Concluding Remarks

- Conservative: Proposed solution procedure maintained GCLs
- Accurate: Obtained up to 5th-order spatial and up to 4th-order temporal convergence for smooth problems
- Robust: Remained monotone/positive for problems with discontinuities

Future/Ongoing Research

- Combine high-order ALE with adaptive mesh refinement
- Apply to multi-material problems

Questions?

Interface Flux Evaluation

- Unique interface flux required at each quadrature point $\vec{x}_q$
- Solve a Riemann problem aligned with $\hat{n}_s$

$$\vec{\mathbf{F}}_q \cdot \hat{n}_s = \mathcal{F}\left[\, \mathbf{U}_{\mathbf{L}}(\vec{x}_q),\ \mathbf{U}_{\mathbf{R}}(\vec{x}_q),\ \hat{n}_s \,\right]$$

- Rusanov (1967) and HLL (Harten, 1983) approximate Riemann solvers

Other Details

High-Order Time Integration

- Explicit multi-stage Runge-Kutta methods

$$\bar{\mathbf{U}}_i^{n+1} = \bar{\mathbf{U}}_i^{n} + \Delta t^n \sum_{j=1}^{s} b_j \mathbf{K}_j$$

- One-, two-, three- and four-stage schemes considered

Determination of Smoothness Indicator

- Step 1: Calculate α

$$\alpha = 1 - \frac{\sum_j \left(P_j^k(\vec{r}_j) - P_i^k(\vec{r}_j) \right)^2}{\sum_j \left(P_j^k(\vec{r}_j) - \bar{u}_i \right)^2}$$

- Step 2: Evaluate $\mathcal{S}$ (inspired by the definition of multiple-correlation coefficients, Lawson, 1974)

$$\mathcal{S} = \frac{\alpha}{\max\left((1-\alpha), \epsilon\right)} \frac{(SOS - DOF)}{(DOF - 1)}$$

- Step 3: Compare to a pass/no-pass cutoff value $\mathcal{S}_c$
  - if $\mathcal{S} > \mathcal{S}_c \Rightarrow$ smooth solution
  - if $\mathcal{S} < \mathcal{S}_c \Rightarrow$ non-smooth solution
  - values for $\mathcal{S}_c$ in the range 1,000-5,000 seem to work well

Behaviour of the Smoothness Indicator

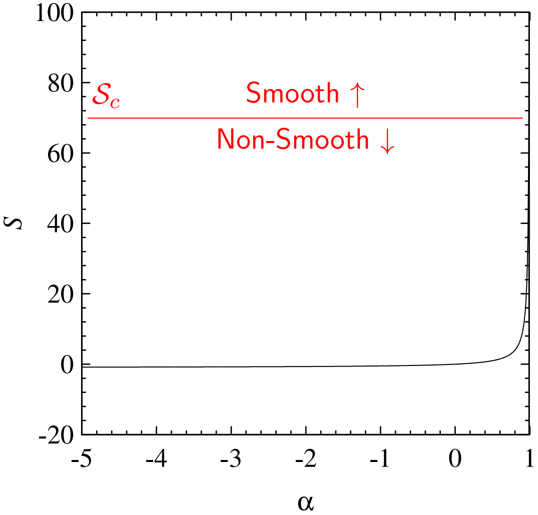

Mesh Smoothing Example

Contours of velocity in $\rightarrow$ direction

No Smoothing

$\varepsilon = 10^{-2}$

$\varepsilon = 10^{-3}$

$\varepsilon = 10^{-6}$

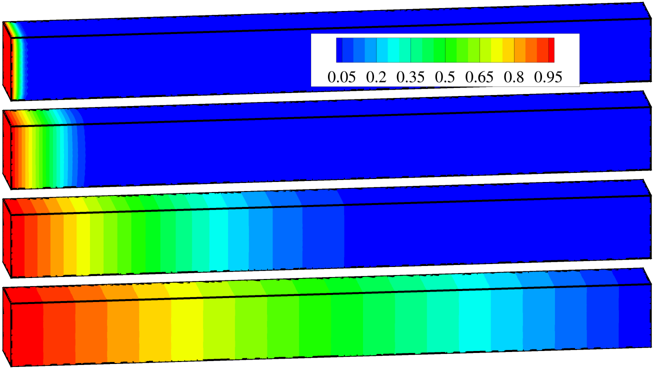

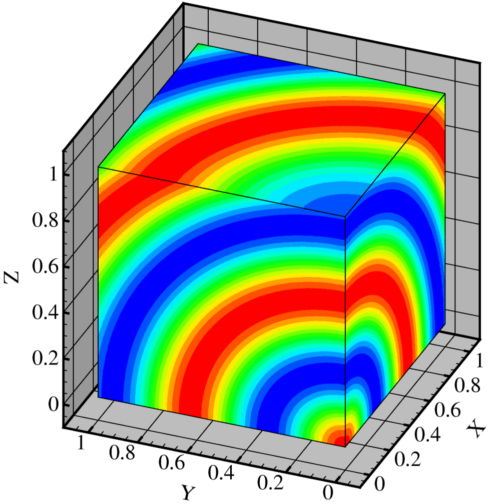

$$u(r) = 1 + \frac{1}{3}\cos 10r$$

$$r = \sqrt{x^2 + y^2 + z^2}$$

$$0 \le x,\, y,\, z \le 1$$

Spherical Cosine - Error Analysis

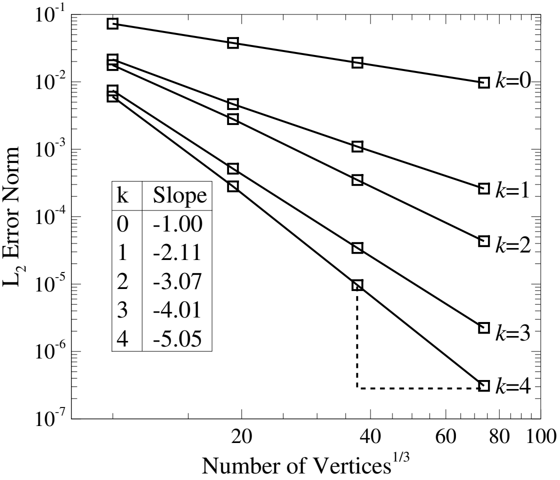

k	Slope
0	-1.00
1	-2.11
2	-3.07
3	-4.01
4	-5.05

Discontinuous Function

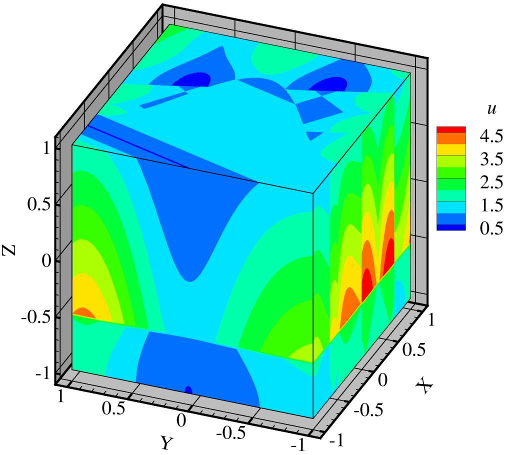

Discontinuities in both:

- $u(x, y, z)$
- $\vec{\nabla} u(x, y, z)$

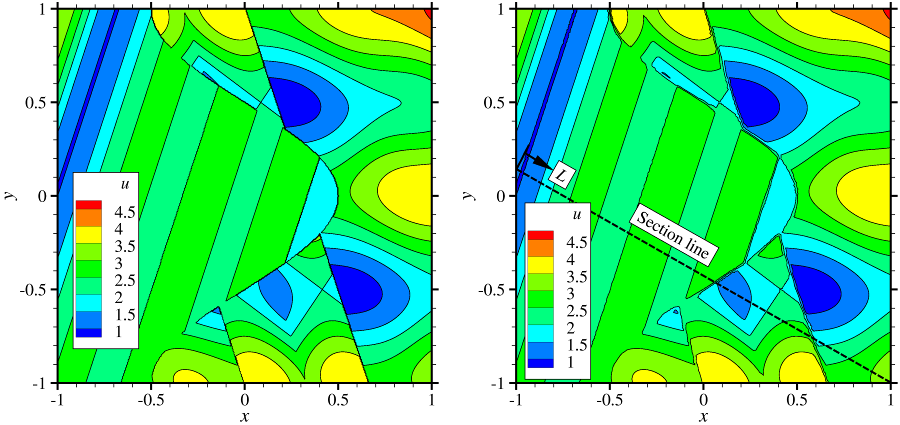

Exact Solution

18M Tetrahedra

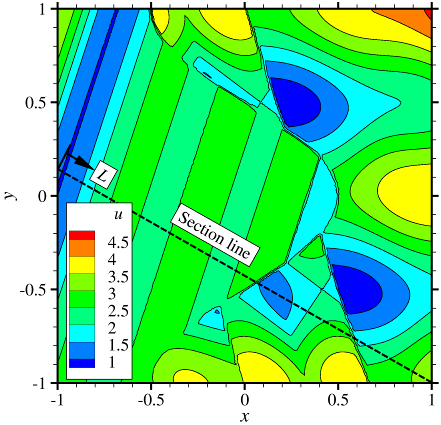

18M Tetrahedra

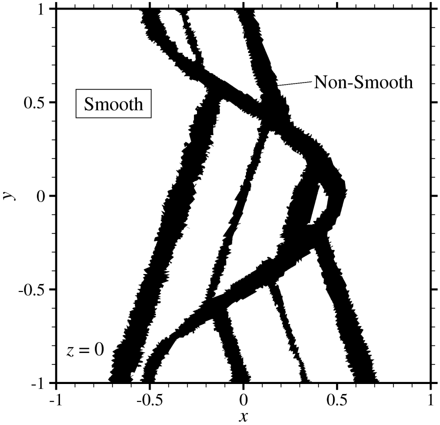

Smoothness Indicator

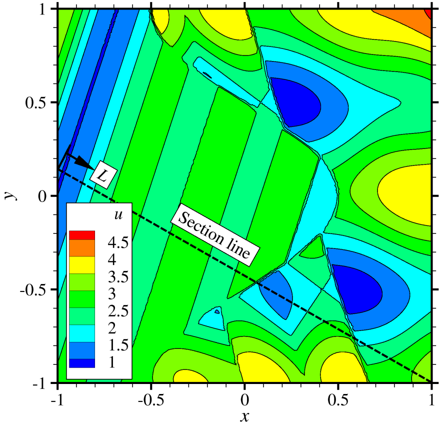

18M Tetrahedra

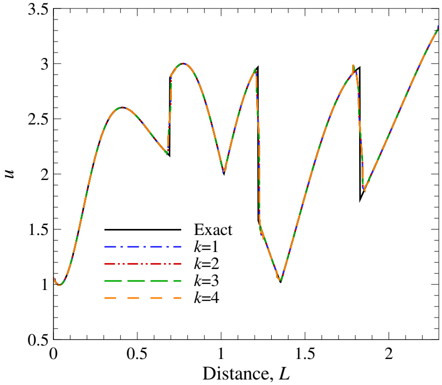

Reconstructed Solution

Preservation of the Free Stream

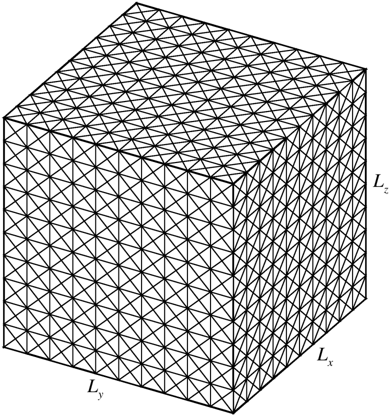

Uniform flow prescribed at time $t = 0\,\text{s}$ with:

$$\rho = 1\,\text{kg/m}^3$$
$$\vec{v} = (2, 2, 2)\ \text{m/s}$$
$$p = 1\,\text{Pa}$$

Integrated in time until $t = 1\,\text{s}$

Preservation of the Free Stream - Mesh Motion

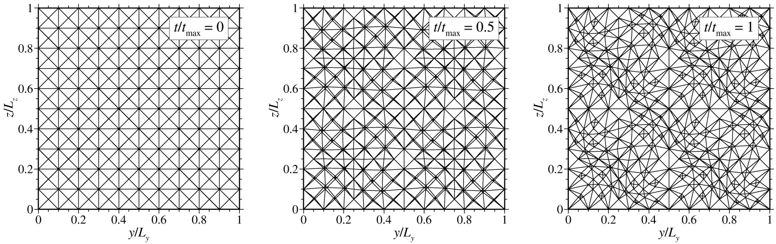

Prescribed sinusoidal grid motion:

$$w_x = A_x L_x \sin\left(f_t t\right) \sin\left(f_x x\right) \sin\left(f_y y\right) \sin\left(f_z z\right) / t_{\max}$$
$$w_y = A_y L_y \sin\left(f_t t\right) \sin\left(f_x x\right) \sin\left(f_y y\right) \sin\left(f_z z\right) / t_{\max}$$
$$w_z = A_z L_z \sin\left(f_t t\right) \sin\left(f_x x\right) \sin\left(f_y y\right) \sin\left(f_z z\right) / t_{\max}$$

Preservation of the Free Stream - Errors

	L_∞ Norm			
Elements	$\boldsymbol{k = 1}$	$\boldsymbol{k = 2}$	$\boldsymbol{k = 3}$	$\boldsymbol{k = 4}$
28,000	6.88×10^{-15}	6.42×10^{-15}	9.14×10^{-15}	9.04×10^{-15}
224,000	7.68×10^{-14}	6.65×10^{-14}	6.34×10^{-14}	8.73×10^{-14}
756,000	3.17×10^{-13}	2.94×10^{-13}	3.53×10^{-13}	3.37×10^{-13}
1,792,000	6.38×10^{-13}	6.38×10^{-13}	5.97×10^{-13}	7.72×10^{-13}

Smooth Supersonic Flow

- Method of manufactured (MMS) solutions used for verification
- Manufactured steady solution of Roy *et al. (2002, 2004)*

$$
\begin{aligned}
\rho &= \rho_0 + \rho_x \sin\left(a_{\rho_x}\pi x/L\right) + \rho_y \cos\left(a_{\rho_y}\pi y/L\right) + \rho_z \sin\left(a_{\rho_z}\pi z/L\right)\\
u &= u_0 + u_x \sin\left(a_{u_x}\pi x/L\right) + u_y \cos\left(a_{u_y}\pi y/L\right) + u_z \cos\left(a_{u_z}\pi z/L\right)\\
v &= v_0 + v_x \cos\left(a_{v_x}\pi x/L\right) + v_y \sin\left(a_{v_y}\pi y/L\right) + v_z \sin\left(a_{v_z}\pi z/L\right)\\
w &= w_0 + w_x \sin\left(a_{w_x}\pi x/L\right) + w_y \sin\left(a_{w_y}\pi y/L\right) + w_z \cos\left(a_{w_z}\pi z/L\right)\\
p &= p_0 + p_x \cos\left(a_{p_x}\pi x/L\right) + p_y \sin\left(a_{p_y}\pi y/L\right) + p_z \cos\left(a_{p_z}\pi z/L\right)
\end{aligned}
$$

- Mach number varying between 3 – 6

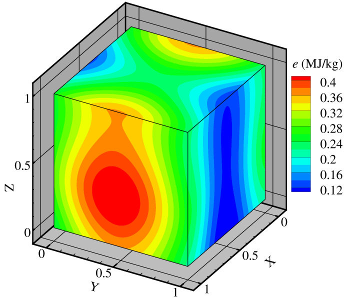

Energy

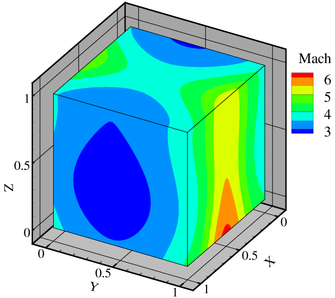

Mach Number

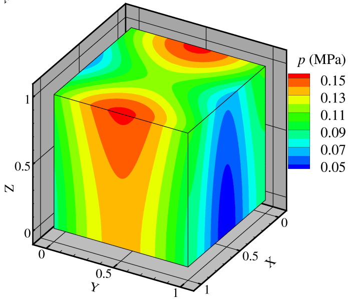

Pressure

Smooth Supersonic Flow - Error Analysis

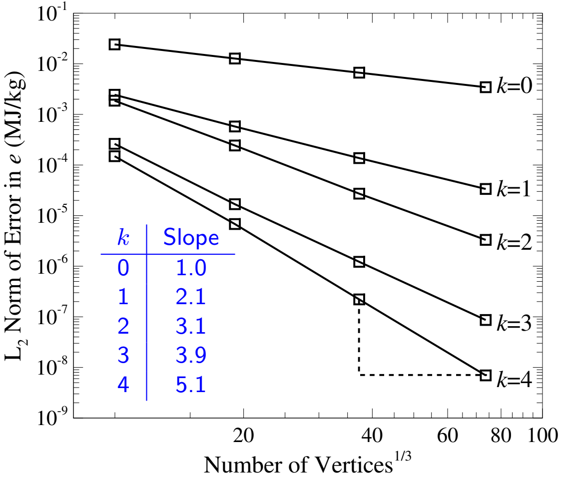

k	Slope
0	1.0
1	2.1
2	3.1
3	3.9
4	5.1

Smooth Supersonic Flow - Computational Efficiency

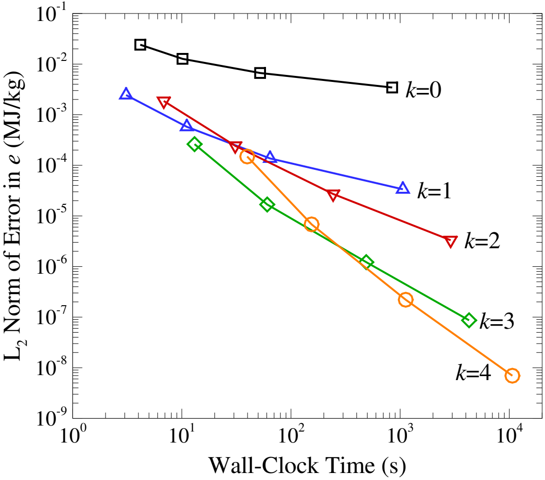

Shock Tube

Initial conditions at $t = 0$ sec:

$$\mathbf{W}(x,0) = \begin{cases} \mathbf{W_L} & \text{if } x \leq 0.5\,\text{m} \\ \mathbf{W_R} & \text{otherwise} \end{cases}$$

where

$$\mathbf{W_L} = \begin{bmatrix} \rho_L \\ u_L \\ p_L \end{bmatrix} = \begin{bmatrix} 1.0 \\ 0.0 \\ 1.0 \end{bmatrix}$$

$$\mathbf{W_R} \begin{bmatrix} \rho_R \\ u_R \\ p_R \end{bmatrix} = \begin{bmatrix} 0.1 \\ 0.0 \\ 0.125 \end{bmatrix}$$

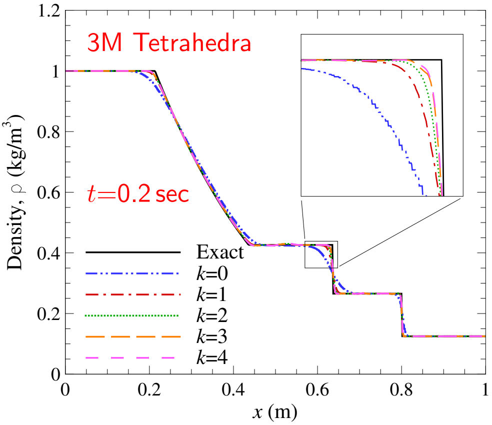

Shock Tube - Error Analysis

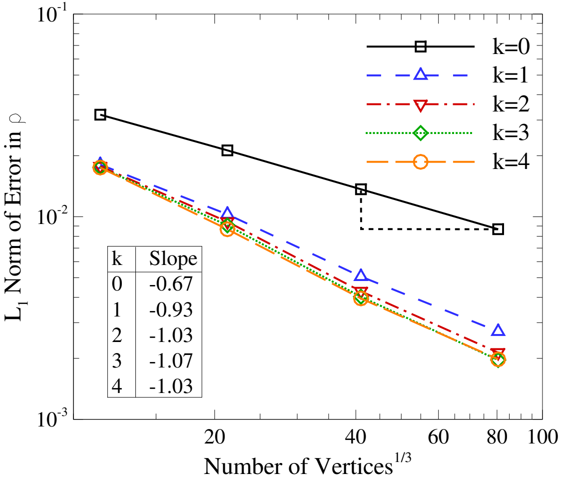

Shock Tube - Computational Efficiency

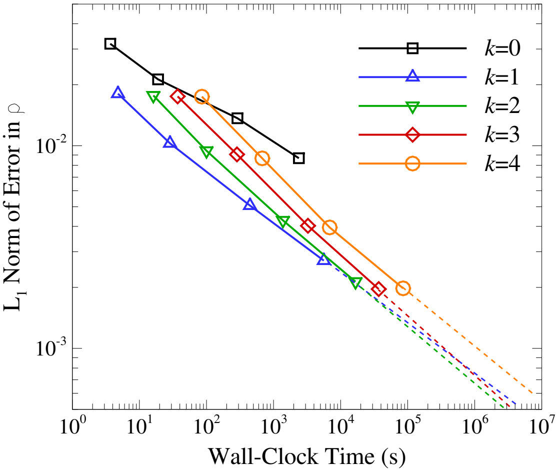

Moving Piston - Reconstructed Density

Reconstructed density at $t = 0.7\,\mathrm{s}$

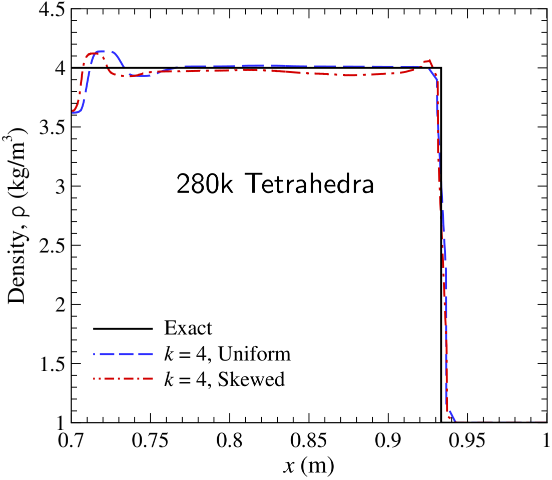

Shu-Osher Prolbem: